2
Fabrication and Characterization Techniques

This chapter includes the synthesis procedure of different 2D and quasi-2D RP perovskites, MoS_2 nanoflakes from its bulk power using liquid phase exfoliation techniques (LPET), MXene nanosheets and nanoflakes from its MAX phase using delamination methods. Moreover, drop-casting as well as spin coating techniques to prepare the thin film. Furthermore, preparation of vertical photodetector as well as lateral photodetector using etching and photolithography techniques respectively are also mentioned. Lastly, investigation of working principles for different characterization techniques such as structural, morphological, electronic, optical and optoelectronic, electrochemical and photo electrochemical. Moreover, it includes physical vapor deposition techniques and photolithography techniques to fabricate the photodetectors.

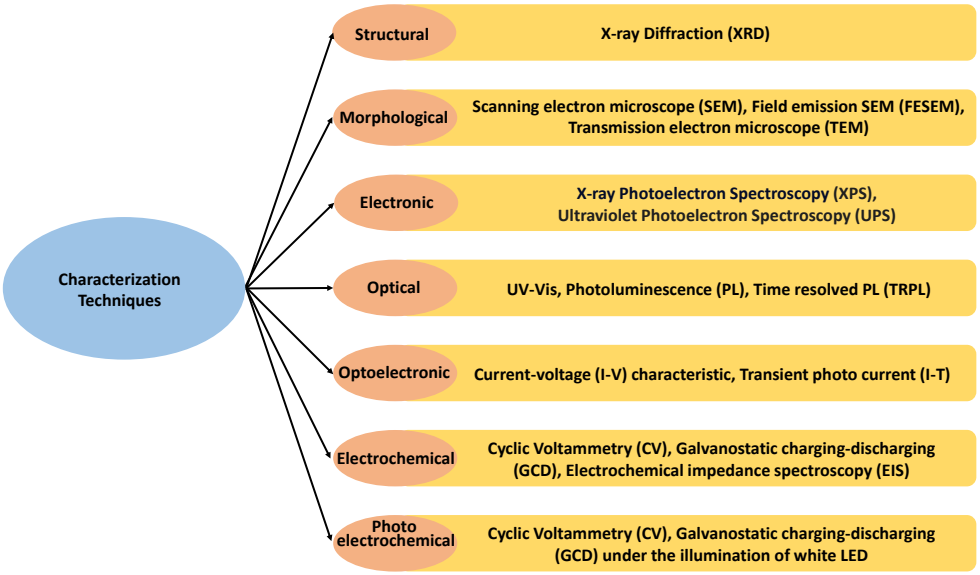


Figure 2.1 Schematic diagram showing different characterization techniques.

2.1 Synthesis process of 2D and Quasi-2D RP perovskites

The synthesis of RP Perovskite material involves two steps and molar concentration of required chemicals in the synthesis process are shown in **Figure 2.2** and **Table 2.1** respectively.

2.1.1 Material Used

Following materials were used to synthesize the RP perovskite materials, MoS_2 nanoflakes, etched MXene, MXene nanosheets, MXene nanoflakes and to fabricate photodetectors, LIBs and Li-PRBs. Lead (II) oxide (PbO, 99.999%; Sigma Aldrich), methylammonium chloride (CH_3NH_3Cl, ≥99.0%; Sigma Aldrich), Formamidine acetate salt ($HN=CHNH_2{\cdot}CH_3COOH$ or $C_3H_8N_2O_2$, 99%; Sigma Aldrich); butylamine ($CH_3(CH_2)_3NH_2$, 99.5%; Sigma Aldrich), 2-(1-Cyclohexenyl)ethylamine ($C_6H_9C_2H_4NH_2$, 97%, Sigma Aldrich), hydriodic acid (HI, 57 wt% in H_2O, distilled, stabilized, 99.95%; Sigma Aldrich), hydrobromic acid (HBr, 48 wt% in H_2O, ≥99.99%; Sigma Aldrich), hypophosphorous acid (H_3PO_2, 50 wt% in H_2O; Sigma Aldrich), molybdenum (IV) sulfide (MoS_2, <2 mm, 98%; Sigma Aldrich), Ti_3AlC_2 (≥90%, ≤40 µm particle size; Sigma Aldrich), Photoresist (PR; S-1813, Microposit), developer (AZ 726 MIF, Merck), orthophosphoric acid (H_3PO_4, 85%; extra pure confirming to IP, BP; LOBA CHEMIE PVT. LTD.), acetic acid (CH_3COOH, Glacial; Qualigens), nitric acid (HNO_3, ACS reagent, 70 %; Sigma Aldrich), reduced graphene oxide (rGO, >98.8%; Shilpa Enterprises), carbon black powder (Super-P, ≥99%; Alfa Aesar), polyvinylidene difluoride (PVDF, Sigma Aldrich), electrolyte (1 M, LiPF6; Alfa Aesar), separator (glass microfibre, Whatman paper GF/D; Cytiva), hydrochloric acid (HCl, ACS reagent, 37%; Sigma Aldrich), 1-methyl-2- pyrrolidinone (NMP, ACS reagent, ≥99.0%; Sigma Aldrich), zinc (dust, <10 µm, ≥98%; Sigma Aldrich), N, N-Dimethylformamide (Anhydrous DMF, amine free, ≥99.9%; Thermo Scientific), Dimethyl sulfoxide (DMSO, 99%; Qualigens), deionized (DI) water, Cu-foil (16 mm diameter; Alfa Aesar), FTO (thickness ≈ 2.3 mm, ≈ 13 Ω /sq; Sigma Aldrich), Si-wafer (4" O100 R1-10 T-P SSP, Macwin), SiO_2 (99.99%, excel instruments), coin cell (CR-2032) and aluminum wire (1.0 mm diameter, 99+%, metal basis; Alfa Aesar).

2.1.2 Synthesis of RP perovskite $(BA)_2(MA)_{n-1}Pb_nI_{3n+1}$, n=1-4

To begin, PbO powder (1116 mg, 5 mM) is dissolved in a solution containing 57% w/w aqueous HI (5.0 mL, 38 mM) and 50% w/w aqueous H_3PO_2 (850 µL, 7.75 mM). The resulting PbI_2 solution of clear bright yellow color is obtained by heating to boiling under 5 minutes of continuous magnetic stirring. The hot PbI_2 solution is used as a stock solution for the synthesis of RP perovskites mentioned below.

$(BA)_2(MA)_3Pb_4I_{13}$ (n = 4): MACl (253.5 mg, 3.75 mM) powder is added the PbI_2 solution which formed black powder precipitate in the solution, which quickly dissolved to give clear bright yellow solution under continuous stirring. In a separate beaker, BA (128 µL, 1.25 mM) is neutralized in an ice bath in 57% w/w aqueous HI solution (2.5 mL, 19 mM) to get BAI solution. Next, BAI solution is added to the clear bright yellow solution of PbI_2/MACl, which resulted in the formation of black precipitate. These precipitates again got redissolved when the combined solution is heated to boiling. The final solution was left to cool at room temperature without stirring, which resulted in the formation of black color rectangular-shaped RP perovskite crystals.

$(BA)_2(MA)_2Pb_3I_{10}$ (n = 3): MACl (225 mg, 3.34 mM) powder is added the PbI_2 solution which formed black powder precipitate in the solution, which quickly dissolved to give clear bright yellow solution under continuous stirring. In a separate beaker, BA (163.5 µL, 1.67 mM) is neutralized in an ice bath in 57% w/w aqueous HI solution (2.5 mL, 19 mM) to get BAI solution. Next, BAI solution is added to the clear bright yellow solution of PbI_2/MACl, which resulted in the formation of black precipitate. These precipitates again got redissolved when the combined solution is heated to boiling. The final solution was left to cool at room temperature without stirring, which resulted in the formation of brown color rectangular-shaped RP perovskite crystals.

$(BA)_2(MA)Pb_2I_7$ (n = 2): MACl (169 mg, 2.5 mM) powder is added the PbI_2 solution which formed black powder precipitate in the solution, which quickly dissolved to give clear bright yellow solution under continuous stirring. In a separate beaker, BA (347 µL, 3.5 mM) is neutralized in an ice bath in 57% w/w aqueous HI solution (2.5 mL, 19 mM) to get BAI solution. Next, BAI solution is added to the clear

bright yellow solution of PbI_2/MACl, which resulted in the formation of black precipitate. These precipitates again got redissolved when the combined solution is heated to boiling. The final solution was left to cool at room temperature without stirring, which resulted in the formation of cherry red color rectangular-shaped RP perovskite crystals.

$(BA)_2PbI_4$ (n = 1): BA (462 µL, 5 mM) is neutralized in an ice bath in 57% w/w aqueous HI solution (2.5 mL, 19 mM) to get BAI solution. Next, BAI solution is added to the clear bright yellow solution of PbI_2 which resulted in the formation of black precipitate. These precipitates again got redissolved when the combined solution is heated to boiling. The final solution was left to cool at room temperature without stirring, which resulted in the formation of yellow color rectangular-shaped RP perovskite crystals.

Separate precursor solution of 0.5M were prepared for all $(BA)_2(MA)_{n-1}Pb_nI_{3n+1}$ (n=1-4) RP perovskites by dissolving perovskites in 60 µl of NMP, which correspond to 25.9 mg for n=1, 44.4 mg for n=2, 63.0 mg for n=3 and 81.6 mg for n=4 RP perovskite. These solutions were used to get the thin films of pristine RP perovskites.

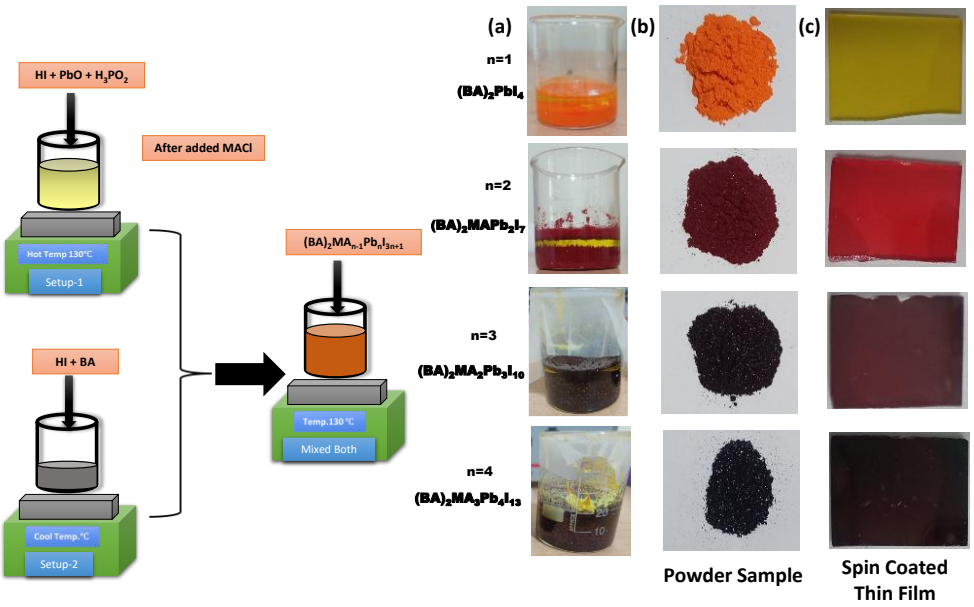


Figure 2.2 (a) Schematic diagram showing different steps in the synthesis of RP perovskite of type $(BA)_2(MA)_{n-1}Pb_nI_{3n+1}$, (n=1-4). (b-c) Camera images for corresponding synthesized powders and thin films.

2.1.3 Synthesis of RP perovskite $(CH)_2(MA)_3Pb_4Br_{13}$, n=4

First, PbO powder (1116 mg, 5 mM) is dissolved in a mixture of 48 % w/w aqueous HBr solution (5 mL, 44 mM) and 50 % aqueous H_3PO_2 (850 µl, 7.75 mM) by heating to boiling at 120 °C under constant magnetic stirring for about 10 min, which formed transparent solution. Next, MACl (440 mg, 5.52 mM) is added which further redissolved under constant stirring to get transparent solution. In separate beaker, 2-(1-Cyclohexenyl)ethylamine ($C_6H_9C_2H_4NH_2$, 144 µl, 0.98 mM) is added dropwise in 48 % w/w aqueous HBr solution (2.5 mL, 22 mM) under constant magnetic stirring in an ice bath so that $C_6H_9C_2H_4NH_2$ disperse uniformly in HBr solution to get CHBr. The solutions of both the beakers are mixed together under constant stirring and yellow precipitates are formed. The stirring was discontinued and the solution is allowed to cool down at room temperature. After extracting the solvents and drying the precipitate, RP Perovskite material in powder form is obtained which is yellow in color.

2.1.4 Synthesis of RP perovskite $(CH)_2(MA)Pb_2I_7$, n=2 and $(CH)_2(FA)Pb_2I_7$, n=2

PbO powder (1116 mg, 5 mM) is dissolved in a mixture of HI (5.0 mL, 38 mM) and H_3PO_2 (850 µL, 7.75 mM) by heating to boiling under continuous magnetic stirring, yielding a clear bright yellow PbI_2 solution. For RP perovskites $(CH)_2(MA)Pb_2I_7$) and $(CH)_2(FA)Pb_2I_7$), MACl (174 mg, 2.57 mM) and

$HN{=}CHNH_2{\cdot}CH_3COOH$ (174 mg, 1.67 mM) are poured respectively into the PbI_2 solution, resulting in the formation of a black powder precipitate. This black precipitate rapidly redissolved, yielding a clear, bright yellow solution upon continuous stirring.

In a separate beaker, 2-(1-Cyclohexenyl)ethylamine ($C_6H_9C_2H_4NH_2$; 300 µL, 2.1 mM) is neutralized in an ice bath with HI solution (2.5 mL, 19 mM) to produce a $C_6H_9C_2H_4NH_2I$ (called as CHI) solution. Subsequently, the solution of $C_6H_9C_2H_4NH_2I$ is introduced to the clear, bright yellow solution of PbI_2+MACl/$HN{=}CHNH_2{\cdot}CH_3COOH$, leading to the emergence of a red precipitate. The precipitates re-dissolved when the mixed solution was heated to boiling. The resultant solution is allowed to cool at ambient temperature without stirring, resulting in the synthesis of RP perovskite material in red color.

Table 2.1 Molar concentration of PbO, H_3PO_2, HX (X=Br, I), MACl, $C_3H_8N_2O_2$ and R-NH_2 for the synthesis of RP perovskite.

Material		First Beaker				Second Beaker	
	n-value	PbO (mg, mM)	H_3PO_2 (µl, mM)	HX (X=Br, I) (ml, mM)	MACl/ $C_3H_8N_2O_2$ (mg, mM)	Alkylamine R-NH_2 (µl, mM)	HX (X=Br, I) (ml, mM)
$(BA)_2(MA)_{n-1}Pb_nI_{3n+1}$, BA=$CH_3(CH_2)_3NH_3$ MA=CH_3NH_3	1	1116, 5	850, 7.75	5, 38	0	462, 5	2.5, 19
	2				169, 2.5	347, 3.5	
	3				225, 3.34	163.5, 1.67	
	4				253.5, 3.75	128, 1.25	
$(CH)_2(MA)_3Pb_4Br_{13}$, CH=$C_6H_9C_2H_4NH_3$ MA=CH_3NH_3	4	1116, 5	850, 7.75	5, 44	440, 6.52	140, 0.98	2.5, 22
$(CH)_2(MA)Pb_2I_7$, CH=$C_6H_9C_2H_4NH_3$ MA=CH_3NH_3	2	1116, 5	850, 7.75	5, 38	174, 2.57	300, 2.10	2.5, 19
$(CH)_2(FA)Pb_2I_7$, CH=$C_6H_9C_2H_4NH_3$ FA= $CH(NH)_2$	2	1116, 5	850, 7.75	5, 38	174, 1.67	300, 2.10	2.5, 19

2.2 Synthesis of MoS_2 Nanoflakes

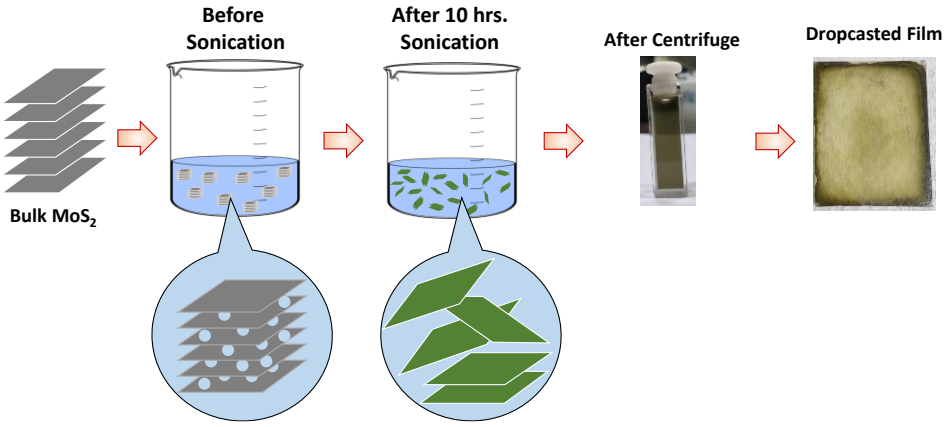


Figure 2.3 Schematic diagram showing synthesis process of MoS_2 Nanoflakes for bulk MoS_2.

Exfoliation of MoS_2 was carried out using LPET. 50 mg bulk MoS_2 powder were added in 10 ml NMP solvent and ultrasonicated for 25 hours. After sonication, the bigger MoS_2 chunks were removed by performing centrifugation at 2000 rpm for 10 minutes, and the tube was left in the stand for 30 mins to further settle the bigger MoS_2 particles. Next, the supernatant suspension was carefully extracted using a micro-pipette. The final concentration of MoS_2 nanoflakes is estimated using microbalance (Sartorius, Model Number: SE2) and found to be ~ 4.12 mg/ml or 25.6 mM. Six

different millimolar concentration MoS_2 solutions (4.2 mM, 8.5 mM, 12.8 mM, 17.0 mM, 21.3 mM and 25.6 mM) were prepared by adding NMP solvent accordingly in such a way that total volume of each MoS_2 solution became 60 µl **(Figure 2.3)**.

2.3 Synthesis process of etched MAX phase, MXene nanosheets and MXene nanoflakes

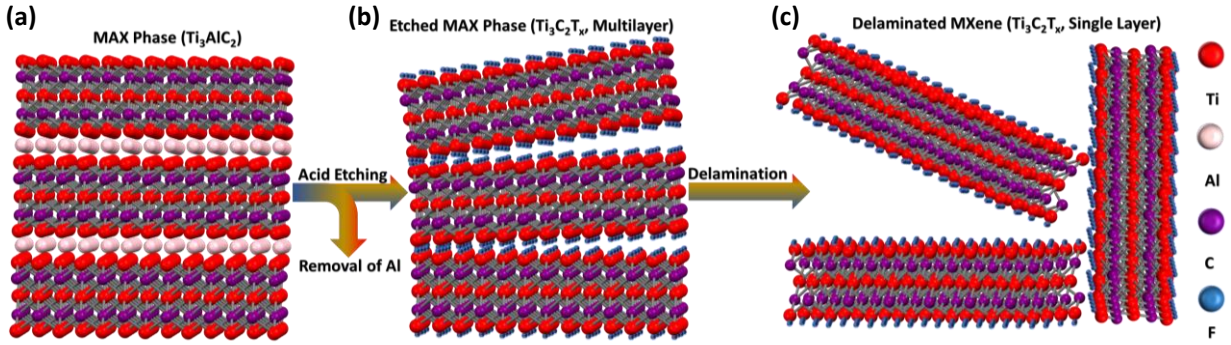


Figure 2.4 Schematic diagram showing synthesis procedure of etched MAX phase and MXene nanosheets.

2.3.1 Synthesis of etched MAX phase

1 gm Ti_3AlC_2 MAX Phase powder is added gradually in 15 ml aqueous HF (40 wt %) under constant magnetic stirring (300 rpm) at 35 °C in a beaker made up of Teflon material and stirred continuously under same rpm for 24 hours. The solution is centrifuged at 10000 rpm for 20 minutes to extract the HF and DI water is added several (~7-8) times in the tube and centrifuged to neutralize the solution (pH ~ 6). When pH level is reached at ~7, the DI water is removed by centrifugation of solution at 10000 rpm for 30 minutes to get precipitate. Finally, etched MAX Phase powder is obtained after drying the precipitate in vacuum oven for whole night at 80 °C **(Figure 2.4a-b)**.

2.3.2 Synthesis of MXene nanosheets

500 mg etched MAX Phase powder in added in 15 ml DMSO, and to start delamination the above solution is kept under constant magnetic stirring (300 rpm) at room temperature for 48 hours. The DMSO is removed after centrifugation (10000 rpm for 15 minutes) of solution several (~5-6) times using DI water. 15 ml DI water is added again and sonicated for 1 hours. The solution is centrifuged at 3000 rpm for 10 minutes and kept for 15 minutes to settle down the bigger size particles. Finally, MXene nanosheets are obtained after collecting the supernatant from the solution **(Figure 2.4a-c)**.

2.3.3 Synthesis of MXene nanoflakes

To obtain the nanoflakes, the supernatant is sonicated for 6 hours under room temperature followed by centrifugation at 1500 rpm for 10 minutes. The solution is left for 15 minutes to settle down bigger sheets. MXene nanoflakes are obtained after collecting the supernatant solution. MXene nanoflakes powder is obtained after centrifugation of supernatant at 15000 rpm for 30 minutes and drying it in vacuum oven at 80 °C for whole night. MXene nanoflakes (5.6 mg) are added in DMF (4 ml) and stirred for 48 hours to make a stable suspension. The final concentration of Ti_3C_2F MXene nanoflakes suspension is 7.5 mM. To vary the concentration of MXene nanoflakes (0.75 mM, 1.5 mM and 2.25 mM) suspensions, the above MXene nanoflake suspension (10 µl, 20 µl and 30 µl respectively) is added in DMF keeping total volume fixed at 100 µl.

2.4 Additive Engineering and their importance

As discussed in chapter 1, the 2D MHPs show interesting photo physical properties with enhanced structural stability against moisture as compared to 3D counterpart, however the

presence of large organic spacer cation results in low device efficiencies which remains a bottleneck for their widespread use as an optoelectronic material. So, additive engineering is an impressive technique to enhance the structural, morphological, optical, and optoelectronic properties with enhanced lifetime of 2D MHP based devices without changing their hereditary properties. In general, the following methods are reported to introduce additives into bulk and 2D MHPs thin films via: (i) one-step precursor solution[Ochoa-Martinez et al., 2021; Xin et al., 2019]; (ii) two-step deposition of the organic sources[Li et al., 2023d; Xin et al., 2020]; (iii) antisolvent[Jin et al., 2023; Khorshidi et al., 2022]; or (iv) post-treatment[Hu et al., 2023; Zhao et al., 2016b]. These first three methods not only retard the rapid crystal growth and aggregation of perovskite crystals at relatively elevated temperatures (e.g., 100–50 ℃) as well as improves the phase stability, moisture resistance and passivates the defects/voids from grain boundaries. On the other hand, the fourth (iv) approach is adopted to passivate the defects because it fills the vacancy and limits the formation of superoxide [Zhang et al., 2020a].

In this thesis, one-step precursor solution method as an additive engineering is explored to enhance the structural, morphological, and optical properties of 2D RP perovskites of type $(BA)_2(MA)_{n-1}Pb_nI_{3n+1}$ (n=1-4) and $(CH)_2(MA)_3Pb_4Br_{13}$ (n=4) using MoS_2 and MXene nanoflakes as an additive and investigated their optoelectronic performance (I-V and I-T using photodetector). These 2D RP perovskites with additives are collectively called hybrids. Moreover, electrochemical and photo-electrochemical performance of the hybrid [$(BA)_2(MA)_3Pb_4I_{13}$ (n=4) + MoS_2] is also investigated using LIBs and Li-PRBs.

2.4.1 Preparation of RP Perovskite-MoS_2 hybrids

Synthesis of RP perovskite $(BA)_2(MA)_{n-1}Pb_nI_{3n+1}$, n=1-4 and MoS_2 nanoflakes are mentioned in **Sub-Section 2.1.2** and **Section 2.2** respectively. The RP perovskite-MoS_2 hybrids for a given n-value of perovskite, is obtained by adding the RP perovskite crystals (0.5M) in the MoS_2 solution (60 µl NMP) of fixed molarity (4.2-25.6 mM). The hybrid solution is sonicated for 15 mins followed by stirring for 20 min at room-temperature. Next, the hybrid solution was immediately used to fabricate thin/thick films.

2.4.2 Preparation of RP Perovksite-MXene nanoflakes hybrids

Synthesis of RP perovskite $(CH)_2(MA)_3Pb_4Br_{13}$, n=4 and $Ti_3C_2T_x$ MXene nano flakes are mentioned in **Sub-Section 2.1.3** and **Sub-Section 2.3.3** respectively. RP Perovskite powder (54.56 mg, 250 mM) is dissolved in 100 µl MXene nanoflakes suspension of 0.75 mM, 1.5 mM and 2.25 mM concentrations. The RP perovskite-MXene hybrid (n=4 + MXene: 0.75 mM, 1.5 mM, 2.25 mM) are obtained by sonication (15 min) of suspension followed by magnetic stirring (30 min).

2.5 Preparation for thin/ drop-casted film

Films (bulk/thin) were prepared on pre cleaned glass substrate. Where, cleaning process includes washing of substrate using sonication in acetone, followed by IPA and DI water for approximately 30 mins each. Moreover, UV-Ozone treatment is also used to enhance the hydrophilic nature of the substrate. Drop-casing and spin coating are the most common techniques to prepare films for material dissolved/dispersed in different solvents.

2.5.1 Drop-casing technique

It is a fairly basic approach for preparing the bulk films in which a given volume (in mM) of liquid-based material is spread uniformly on the substrate and then annealed on a hot plate at a controlled temperature for a set period of time until all solvents have not evaporated. The thickness of the films depends on the molar concentration of material for a fixed volume of solvents. The camera image for drop-casted film of MoS_2 nanoflakes is shown in **figure 2.3**.

2.5.2 Spin coating technique

It is a method of preparing a thin film in which liquid-based materials are coated at a given revolution per minute (rpm) for a set time on a substrate using a spin coater. This process produces

considerably more uniform films than the previous technique. It incorporates centripetal force and the surface tension of the liquid-based material during the spinning process. Single or multiple step spinning programs such as 600 rpm for 15 seconds and/or 3000 rpm for 30 seconds, are programmed in the spin coater before the substrate is placed on the coater's chuck. Now, the solution is spread on the substrate and after spinning the coater for the specified rpm and time, the material is uniformly coated on the substrate. Finally, spin coated films are annealed at a regulated temperature (50 $^{\circ}$C for 30 min in ambient air and at 100 $^{\circ}$C for 30 mins inside an Argon atmosphere glove box) to evaporate the leftover solvents, resulting in thin films. The camera images for spin coated thin films are shown in **figure 2.2c**.

2.6 Physical Vapor Deposition (PVD) technique

It is a technique to transform the target (i.e., solid materials) into vapor form using heat (thermal vapor deposition), electron-beam (electron-beam deposition) and plasma (sputtering) under low pressure less than 7.5 X 10^{-5} Torr. These vapors are deposited on the substate to make a thin film of material. The real time of deposition is expressed in Å/sec and uniformity of the thin films depends on the distance between target and substrate, substrate rotation as well as deposition angle. SiO_2 and Al metal thin films are deposited by e-beam deposition **(Figure 2.5)**.



Figure 2.5 Camera image for e-beam deposition system from Excel Instruments.

2.7 Preparation of photodetector

This thesis includes two types of photodetectors, vertical and lateral. Preparation of both types of photodetectors are mentioned below.

2.7.1 Vertical Photodetector

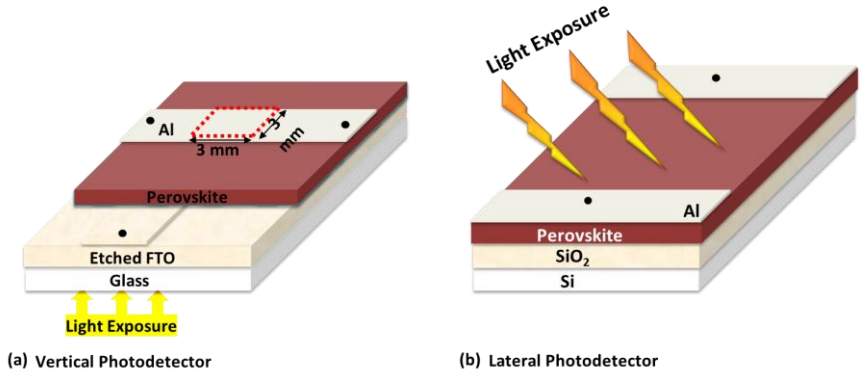


Figure 2.6 Schematic diagram showing the photodetectors (a) vertical and, (b) Lateral configurations

2.7.2 Lateral Photodetector: The lateral photodetectors were prepared on SiO_2 coated Si-substrate using photolithography techniques **(Figure 2.6b)**.

The vertical configuration photodetectors were prepared on fluorine-doped tin oxide (FTO) glass substrate (25 × 10 mm^2, thickness ~ 2.3 mm, ~ 13 ohms/sq). The middle portion of FTO is covered by the Kapton tape strip (3 mm width) and the remaining FTO was etched by using HCl acid and Zn-dust. Now, perovskite material is coated on pre cleaned etched FTO substrate using drop-casting or spin coating techniques as mentioned in section 2.6. The Al metal electrodes of 100 nm thickness were deposited on the perovskite films by thermal vapour deposition technique using a shadow mask (slit width 3 mm) to form the vertical configuration photodetector (Al/Perovskite/FTO). All the photodetectors were made with a 9 mm^2 (3×3 mm^2) active area **(Figure 2.6a)**.

2.7.1.1 Photolithography

It is a technique to fabricate electronic/optoelectronic devices with small feature size adopting etching/lift off methods to investigate the optoelectronic properties of MHPs. It involves light, such as visible light, deep ultraviolet light, or ultraviolet light to transform the desired pattern on a SiO_2 coated Si wafer. The smallest feature size (D_{min}) that can transform on wafer is determined by the numerical aperture of the lens as observed from the wafer and the wavelength (λ) of light used.

$$\mathbf{D_{min} = k_1 \times \frac{\lambda}{Numerical\ Aperture}} \qquad (2.1)$$

Where k_1= ~0.4 is a process-related coefficient that depends on the incident light intensity distribution and the angle at which light strikes a reticle.

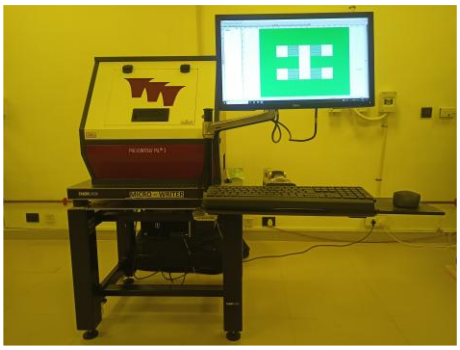


Figure 2.7 Camera image for micro-writer system (MicroWriter ML ®3) from Durham Magneto Optics.

The depth of focus (D_f) is a constraint in modern systems, limiting both the photoresist thickness and the depth of topography on wafer.

$$\mathbf{D_f = k_2 \times \frac{\lambda}{(Numerical\ Aperture)^2}} \qquad (2.2)$$

Where, k_2 is another process-related coefficient.

2.7.1.2 Photoresist (PR)

It is a light sensitive material used in lithography techniques to transform the pattern on substrate such as SiO_2 coated Si-wafer. Conversional PR consists of three components resin (resin is a binder that provides the adhesion with substrate,), sensitizer (photoactive substance), and solvents (to keep PR in liquid form). There are two types of PR: (1) Positive PR (2) Negative PR

Positive PR: It is a type of PR where the exposed part is soluble, whereas unexposed part is insoluble in developer (**Figure 2.8**).

Negative PR: It is a type of PR where the exposed part is insoluble, whereas unexposed part is soluble in developer in developer (**Figure 2.8**).

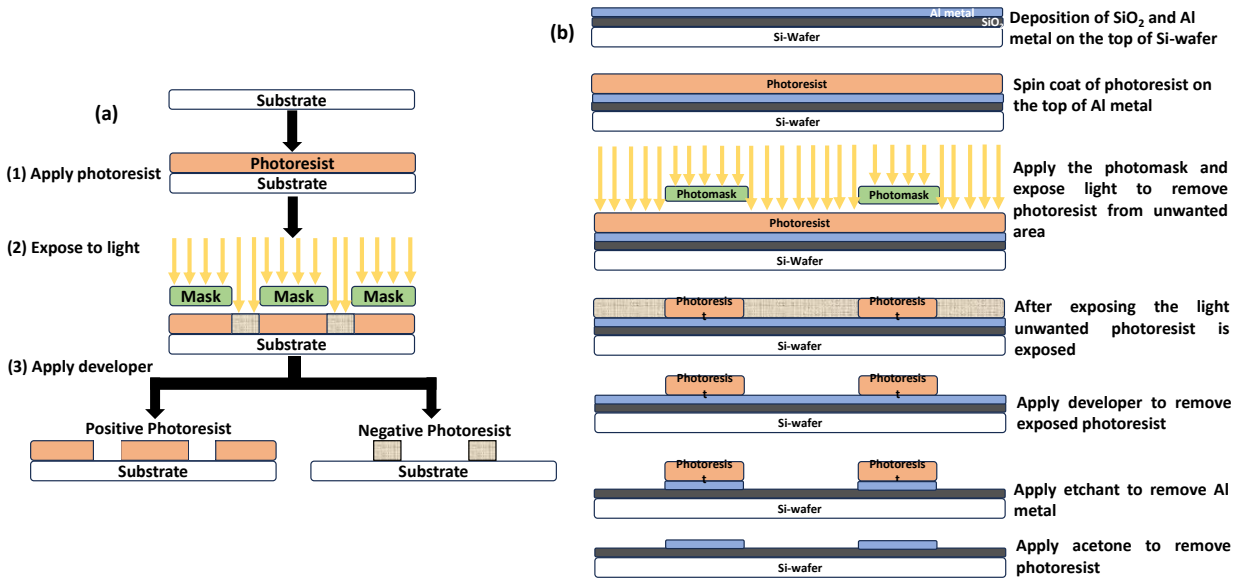


Figure 2.8 (a) Schematic diagram showing the use of positive and negative PR in photolithography technique. (b) Schematic representation shows different steps involved in transforming pattern on SiO_2 coated Si-wafer.

2.7.1.3 Preparation of pattern to fabricate photodetector: It involves several steps which are mentioned below.

- **i.** First, I prepared a device pattern using CleWin5 software and then inverted it to expose the unwanted area of substrate.
- **ii.** Deposit 100 nm SiO_2 and then 100 nm Al metal on clean Si-wafer (4'' O100 R1-10 T-P SSP) using e-beam deposition. (Note: Wafer is at room temperature throughout the deposition).
- **iii.** Spin coat the positive photoresist (PR; S-1813) on the top of Al metal at the rpm of 4000 for 30 second under lowest light condition.
- **iv.** PR coated wafer was prebaked at 105 °C on the hot plate for 1 minute to remove the excessive solvents from PR.
- **v.** Expose the PR coated wafer using h-line (405 nm) microwriter (**Figure 2.7**) as per our desired pattern as shown in **figure 2.8b**. Exposure of light using microwriter weakens the polymer/PR over the area shown with bule color in **figure 2.8b** so that it can be more soluble in developer (AZ 726 MIF).
- **vi.** Dip the wafer in the developer for 40 sec at room temperature to dissolve the weakened PR and then again post baked the wafer at 110 °C on the hot plate for 1 minute to get exact copy of pattern on the wafer.
- **vii.** Now prepare the etchant for Al metal with the help of orthophosphoric acid (85%; extra pure confirming to IP, BP; LOBA CHEMIE PVT. LTD.), acetic acid (Glacial; Qualigens), nitric acid (ACS reagent, 70 %; Sigma Aldrich) and deionized water (DI) in a ratio of 16:1:1:2 respectively. Here, first we added 48 ml orthophosphoric acid and then 3 ml acetic acid. After that pour 3 ml nitric acid drop by drop into the solution of orthophosphoric acid and acetic acid. Finally, DI is added into the solution to dilute it and stirred the whole solution for 30 minutes at 60 °C.
- **viii.** Dip the wafer into the solution of etchant for 43 seconds and shake continuously to etch the Al metal from the exposed area.
- **ix.** Finally, dip the wafer in the acetone for 15 minutes to remove unexposed PR to get device electrode followed by IPA (5 minutes) and water (5 minutes).
- **x.** FESEM image for device electrode is shown in **figure 2.9a**.
- **xi.** The required pristine or hybrid RP perovskite solutions were spin-coated at 3000 rpm for 30 seconds under ambient air conditions, followed by post annealing at 70 °C for 20 minutes in ambient air conditions. **Figure 2.9b** shows the uniform coverage of perovskite material between channels.

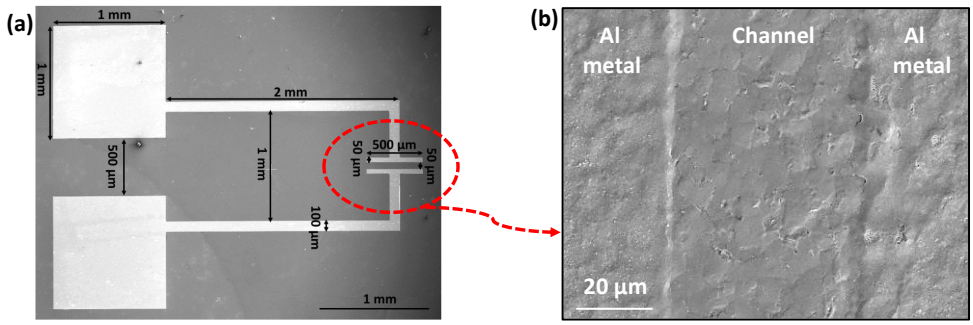


Figure 2.9 (a) FESEM image for photodetector electrode prepared using photolithography (b) Uniform coverage of perovskite material between channel using spin coating method.

2.8 Structural Characterization

powder X-ray diffraction was used to investigate the structural properties of the material.

2.8.1 X-ray powder diffraction (XRD)

It is the most widely used non-destructive analytical technique to determine the crystal structure, phase identification, crystallite size, lattice strain of the crystalline sample (thin/drop casted film or power).[Cappella et al., n.d.] The working principle of XRD is based on Bragg's Law which states that when X-rays are diffracted from two successive planes, constructive as well as destructive interference takes place and X-ray diffraction pattern are obtained only when diffracted X-rays interfere constructively only i.e., diffracted x-rays must be in same phase **(Figure 2.10a-b)**.

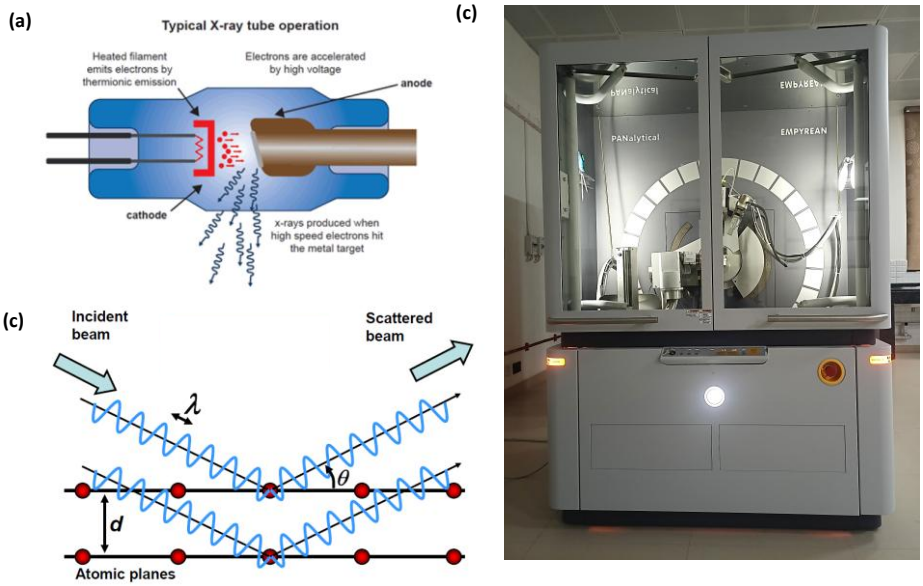


Figure 2.10 (a) Schematic representation showing generation of X-ray (b) Schematic representation of X-ray showing interaction with lattice planes[Nasir, 2018]. (c) Camera image for XRD system from PANalytical (EMPYREAN).

Bragg's law can be written as,

$$2d_{hkl} \sin\theta = n\lambda \qquad (2.3)$$

Where d is the interplanar spacing between two consecutive planes. h, k, l are the miller indices of the different planes. 2θ is the diffraction angle of X-rays from two consecutive planes with respect to the incident X-rays. n=1, 2, 3, 4...∞. Where n=1 means first order diffraction and so on. λ=0.1542 Å is the wavelength of incident characteristic X-rays produced by Cu K_α-radiation.

Sample Preparation: Thin films or drop casted films were prepared over glass slides and measurements are performed on Rigaku-Smart Lab XRD using Cu Kα (λ = 0.1542 nm, 25 kV, 40 mA) X-rays and diffraction angle step size of 0.2° in glancing angle mode.

2.9 Morphological Characterizations

Scanning electron microscopy (SEM)/field emission scanning electron microscopy (FESEM), transmission electron microscopy (TEM), and atomic force microscope (AFM) were used to investigate the surface morphology of the material.

2.9.1 SEM/FESEM

A SEM/FESEM produces the image as well as elemental composition of any sample (metal, semiconductor, and insulator) using raster scanning pattern with highly focused electron beam. This material can be thin films or in power form. Here electron beams are emitted using two types of emitters: (1) Thermionic emitters (2) field emitters.

Conventional SEM works on the thermionic emission principle where electric current is applied to heat up the filament which is made up of tungsten (W) or lanthanum hexaboride (LaB_6). As a result, electron-beam is drawn from a thermionic gun and acts as cathode. LaB_6 and W filament have a diameter of about 20 μm and 100 μm respectively. Due to the lower work function of LaB_6 (~2.65 eV) and CeB_6, this filament produces electrons with better brightness as compared to W (~4.5 eV) leading to record brighter images. Whereas Field emission SEM works on the field emission principle i.e., here, electron beams are drawn from field emission gun after applying high electric filed of the order of $2\text{-}7 \times 10^9$ V/m to the cathode made up of tungsten single crystal of diameter ~100 nm. The field emission gun emits the brightest, most coherent electron beams, enabling the highest resolutions as compared to conventional SEM. The most common accelerating voltage used in SEM/FESEM to accelerate the electron-beams ranges from 0.5 kV to 30 kV. Electron-beams accelerated at high volage have shorter wavelengths and hence provide better resolution of the image. Magnetic and objective lenses control electron-beam diameter and focus them right to the samples.

When the e-beam interacts with the sample, secondary electron, backscattered electrons and X-rays are generated which are detected by secondary detector, backscattered detector and X-ray detector **(Figure 2.11a)**.

i. **Secondary electron:** These electrons are generated from the outermost shell of the atoms existing in the sample. These are low energy electrons of the order of 50 eV as they escape only from the top surface of sample of about few nanometers and provide three dimensional features of the sample.

ii. **Backscattered electron:** These are the primary electrons backscattered at the right angle from the different nucleus of the atom existing in the sample due to elastic collisions. These electrons detect contrast between areas with different chemical compositions.[Burany, 2003] It is also used to investigate the crystallographic structure of the sample as they form electron backscatter diffraction image.

iii. **X-rays:** When electron beams interact with the sample, it knocks out electrons from the innermost shell of the atoms existing in the sample and creates vacancies in the corresponding shell. Such vacancies are filled by just outermost electrons and x-rays are produced. These X-rays are detected by X-ray detector and provide the weight % or atomic % for different elements in the sample.

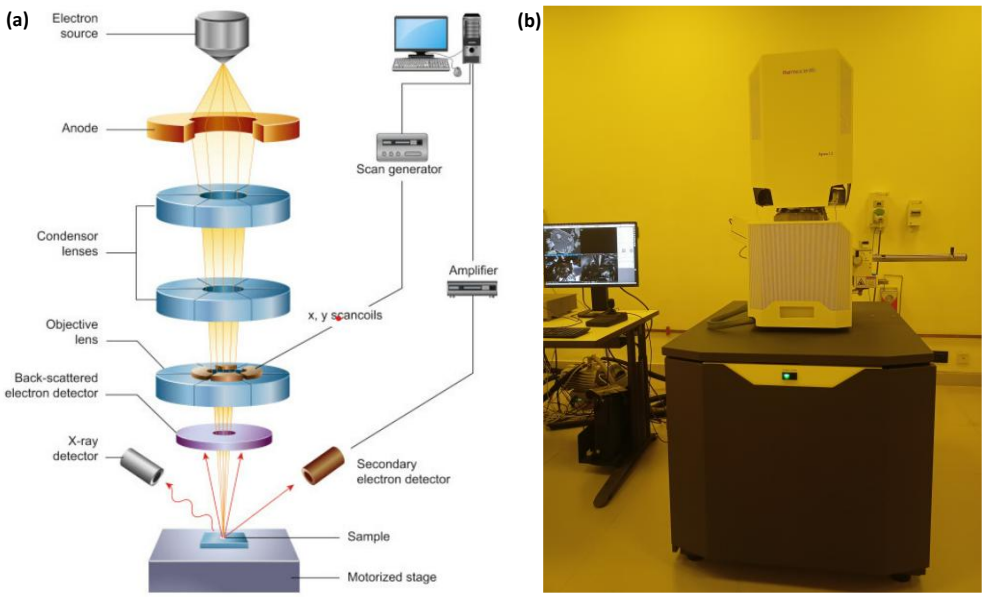


Figure 2.11 Schematic representation showing the working principle of SEM/FESEM ["https://www.nanoscience.com/techniques/scanning-electron-microscopy/," n.d.]. (b) Camera image for FESEM from thermoscientific (Apreo 2 S).

Sample Preparation: Thin or dropcasted films are prepared over glass slides or FTO. An ultra-thin electrically conducting materials such as gold-palladium is sputtered under vacuum conditions to make its surface conducting. Next, samples are electrically grounded with stub at sample stage using double sided carbon tape to prevent the accumulation of electrostatic charge on the sample [Stokes, 2008]. Apreo 2 S FESEM systems from thermoscientific is used to investigate the surface morphology as well as cross-sectional view of the samples **(Figure 2.11b)**. Moreover, EDAX are recorded using Zeiss EVO 18 Special Edition model.

2.9.2 Transmission electron microscopy (TEM)

TEM works on the transmission of highly energetic electron beams through very thin samples under high vacuum. It gives better resolution less than 1 nm, allowing us to examine the columns of atoms, dislocations, and defects in crystalline samples, as well as the molecular machinery found within cells. Images of the sample are captured on the digital screen, which contains a sensor like CCD, a layer of photographic film, or a fluorescent screen [Munir et al., 2021].

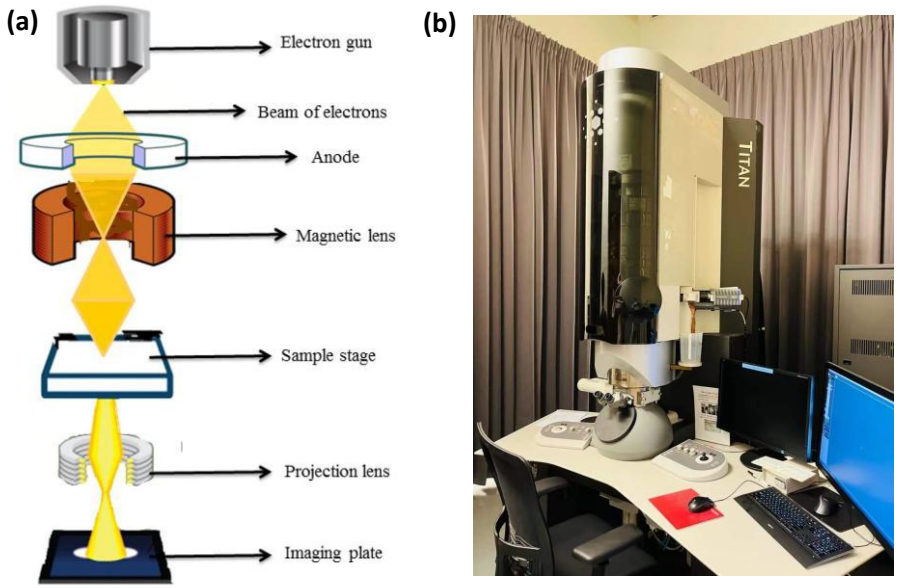


Figure 2.12 (a) Schematic diagram showing working mechanism of TEM [Munir et al., 2021]. (b) Camera image for TEM system (Titan ST).

The image appears dark in areas of the sample where electrons cannot pass through the material. Whereas the image appears brighter where electrons are transmitted, with an array of greys in between, depending on how the electrons interact with and are transmitted by the sample.

Sample Preparation: The lattice structure was studied by HRTEM using Titan ST operating at 300 kV. The dispersed MXene nano flakes were dropcasted on the Cu grid to prepare the sample to record the imaging.

2.9.3 Atomic Force Microscope (AFM)

AFM is a type of scanning probe microscopy (SPM) used to investigate three-dimensional topography of thin films with high contrast i.e., height and roughness of the deposited material can measure directly here. It also can measure the surface properties like surface potential, surface temperatures, magnetic fields, and other physical properties. It has the ability to operate in ambient air, vacuum and liquids and doesn't need to sputter the surface of the sample with metal as in case of SEM/FESEM. The AFM has a resolution of a fraction of a nanometer. An image of the sample is obtained in this instance by quantifying the force between the probe's tip and the sample. A major part of AFM is (1) cantilever (2) support for cantilever (3) piezoelectric element made up of ceramic material to oscillate the cantilever at its eigen frequency (4) tip acts as probe (5) detector (6) drives to move the sample as well as tip in x, y and z directions [Microscope, 1988] **(Figure 2.13a)**. Here, the detector measures the deflection of cantilever with respect to the equilibrium position and converts it into electrical signal. The equipment operates in three distinct modes as per the nature of tip movement: (1) contact mode (2) non-contact mode (2) tapping mode [Cappella et al., n.d.].

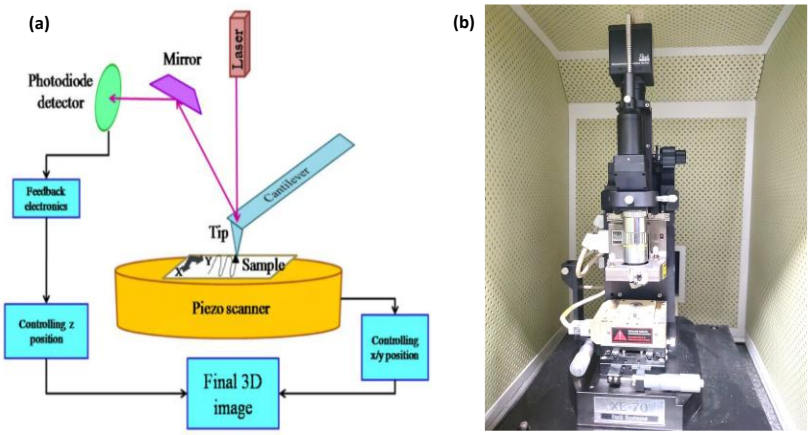


Figure 2.13 (a) Schematic representation showing basic working principle of AFM [Bangalore et al., 2018]. (b) Camera image for AFM (Park Systems XE-70 model).

i. **Contact Mode:** An image of the deposited material is produced by dragging the tip of the cantilever across the surface of the sample. In this case, the surface of the sample needs to be uniform to prevent tip damage. After the characterization, the sample suffers degradation effect.

ii. **Non-contact Mode:** In this mode, tip of the cantilever does not touch the surface of the sample i.e., oscillate just above the sample with its resonant frequency or just above the amplitude modulation to generate the image. The oscillation's amplitude is between few picometer to a few nanometers (less than 10 nm). When the cantilever tip interacts with the sample, van der Waal force acts on it. Here, the tip as well as sample doesn't suffer degradation effect **(Figure 2.13b)**.

iii. **Tapping Mode:** In this mode, the tip of the cantilever oscillates up and down with its resonant frequency. Where the oscillation's amplitude ranges from a few nanometers to 200 nanometers. When the cantilever tip interacts with the sample, several forces such as

electrostatic force, van der Waal force, and dipole-dipole interaction act on it. Here, the tip as well as sample suffer degradation effect.

Sample preparation: Thin films or dropcasted films were prepared over glass slides.

2.10 Electronic characterization

X-ray Photoelectron Spectroscopy (XPS) and Ultraviolet Photoelectron Spectroscopy (UPS) characterizations were investigated the electronic properties of the material (bulk/thin film or powder). These techniques are based on photoelectric effect. Where electrons are ejected under X-ray/ultra-violet photon illumination.

2.10.1 X-ray Photoelectron Spectroscopy (XPS)

It is a quantitative technique not only used to identify elemental composition of atoms that exist on the surface of sample (~10 nm), but also other elements bonded to. Moreover, electronic state of different atoms within the material is investigated using this technique. Here core shell electrons are ejected from the atoms in a sample under X-ray photon illumination to investigate the binding nature of atoms **(Figure 2.14a-b)**.

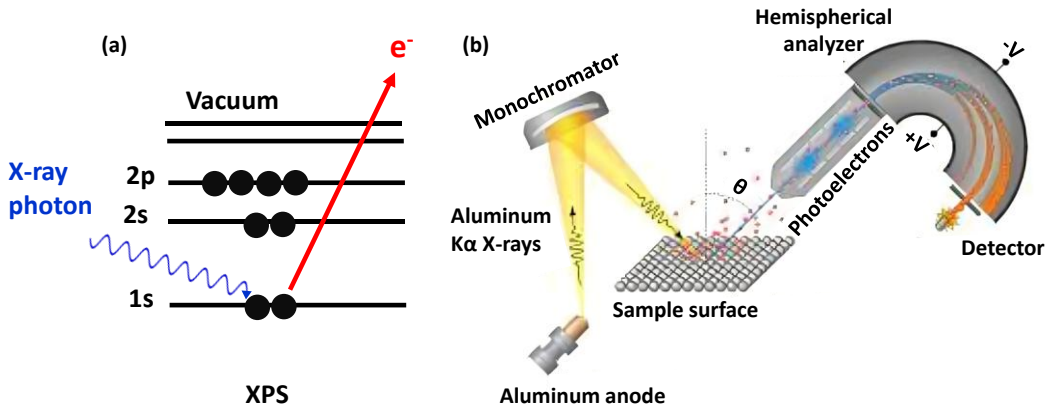


Figure 2.14 (a) Schematic diagram showing the ejection of electrons from core shell of atoms under X-ray photon. (b) Schematic diagram showing the working mechanism of XPS (Kratos Analytical Ltd, Model: AXIS Supra^{+}) [Rocha et al., 2018].

Note: When the atoms of dopant material donate their electrons to the atoms of host material due to their lower electronegativity, then the core electrons of atom in the host sample experience reduced effective nuclear charge due to screening effect. As a result, binding energy of photoelectrons is reduced. In this case oxidation state of atoms lowered, and we get negative shift in binding energy in the XPS spectrum and vice versa.

Sample Preparation: Thin films were prepared over glass slides. Next samples were mounted on stub using carbon tape and measurements were performed using XPS Surface Analysis Instrument (Kratos Analytical Ltd, Model: AXIS Supra^{+}). Al k_{α} is used as X-ray source with a photon energy of 1486.6 eV **(Figure 2.14c)**.

2.10.2 Ultraviolet Photoelectron Spectroscopy (UPS)

It is a technique to examine the density of states of electrons near the valence band edge. Here the outermost electrons are ejected from the atoms in a sample under the illumination of ultra-violet photon **(Figure 2.15a-b)**. Photoelectrons are produced from a material under high vacuum only when the energy of the incident X-ray photons exceed the binding energy of the material, as demonstrated by **equation 2.4**.

$$E_{kinetic\ energy} = E_{incident\ energy\ (h\nu)} - E_{binding\ energy} - \Phi \qquad (2.4)$$

Where, ν is the frequency of incident photons. Moreover, $E_{kinetic\ energy}$, $E_{incident\ energy\ (h\nu)}$, $E_{binding\ energy}$ and Φ is the kinetic energy of ejected electrons, incident energy of photons, binding energy of ejected electrons and work function of ejected electrons respectively. Φ is the energy difference between vacuum energy level and fermi level of a material.

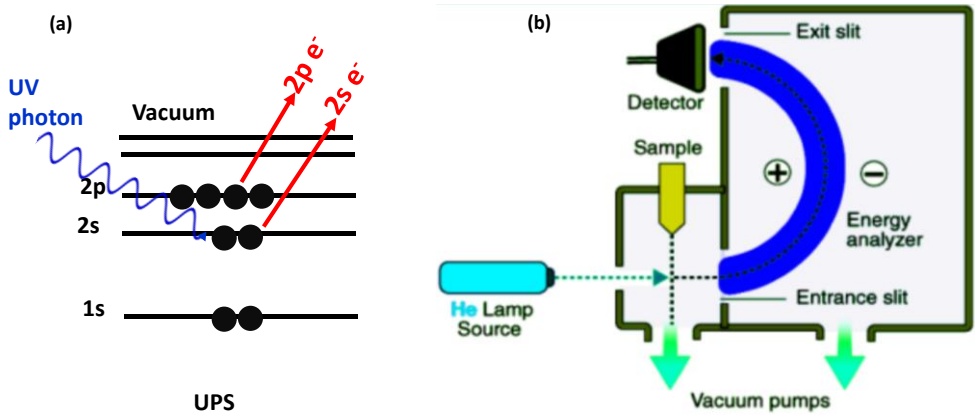


Figure 2.15 (a) Schematic diagram showing the ejection of electrons from the outer shell of atoms in under ultraviolet photon illumination. (b) Schematic diagram showing the working mechanism of UPS ["https://testbook.com/chemistry/photoelectron-spectroscopy," n.d.].

Sample Preparation: UPS measurements were performed in an ultra-high vacuum (UHV) ScientaOmicron multi-probe system operating at a base pressure of 10^{-10} mbar. Samples were prepared by drop-casting on indium tin oxide (ITO) and contacted to the sample plate with molybdenum strips for electrical contact with the analyzer. UPS was measured at an electron take-off angle normal to the sample surface with a 10 V bias applied between the ground to observe the secondary electron cutoff **(Figure 2.17c)**. A partially attenuated 21.2 eV vacuum UV (He 1 source) (HIS-13 focus) and an Argus CU electron analyzer were used. All scans were acquired with a pass energy of 2 eV and analyzed applying linear extrapolation to determine the VBM and the secondary electron cut-off.

2.11 Optical Characterizations

The optical characterization technique is a low-cost, fast, facile, non-contact and non-destructive technique to determine the optical properties of sample properties like absorbance, reflectance, transmittance, film thickness, and optical constants etc. This technique allows the sample (thin film, power in the form of pallet or liquid) to be reused for further processing or analysis.

2.11.1 Ultraviolet-Visible (UV-VIS) Spectroscopy

The UV-VIS spectroscopy is performed with the help of UV-VIS Spectrometer. It majorly measures the amount of light absorbed (A) or reflected (R) by the semiconducting sample in UV and visible region (wavelength: 200-800 nm) of electromagnetic spectrum. In this spectroscopy molecules of a given sample undergo electronic transition from highest occupied molecule orbital (HOMO) to lowest unoccupied molecular orbital (LUMO) at a specific wavelength of given spectral region which resulted in the optical bandgap of the material. The working mechanism is shown in **figure 2.16a.**

It is also used to investigate the elemental concentrations quantitatively for a given solution according to Beer–Lambert law:

$$\mathbf{A = \varepsilon Cl = \log_{10}\left(\frac{I_0}{I}\right) = \log_{10}\left(\frac{1}{T}\right) = -\log_{10}(T)} \qquad (2.5)$$

$$A + R + T = 1 \qquad (2.6)$$

Where, I_o is the intensity of light passed through reference/blank sample, I is the intensity transmitted through material. So, (I_o-I) is the intensity of light absorbed by the sample considering no light is reflected. Ɛ (in liter/mol-cm unit) is the molar extinction/absorption coefficient for each material. It is the intrinsic quantity of each material and determines how strongly a material absorbs a particular wavelength of light. c (in mol unit) is the concentration of the material in each solution and l (in cm unit) is the length of path travelled by light for the given solution.

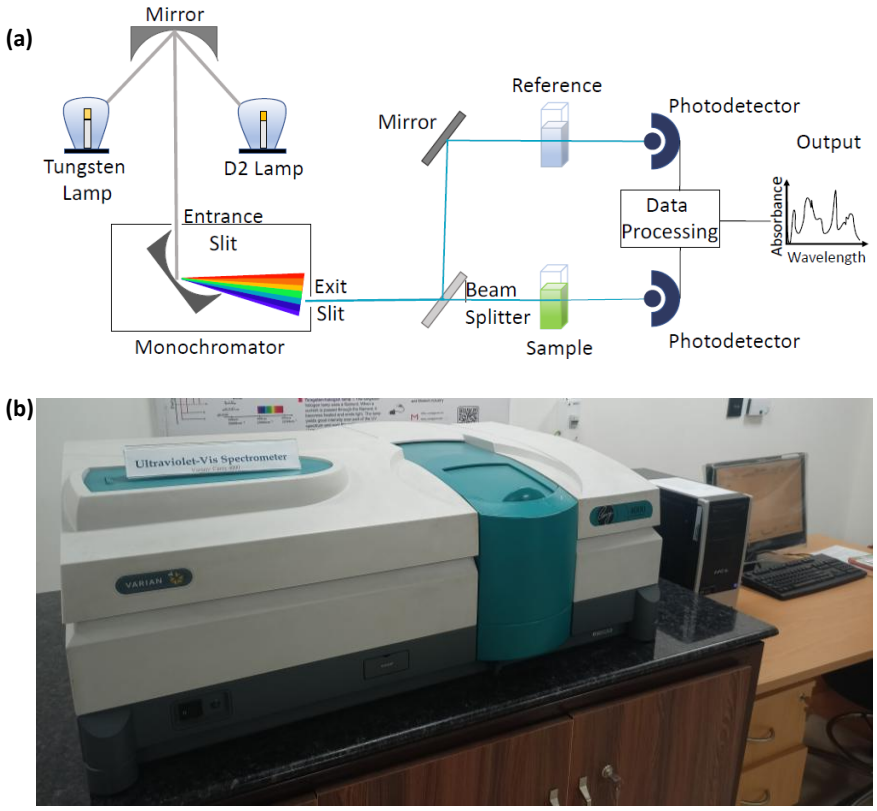


Figure 2.16 (a) Schematic representation showing working principle of UV-Vis spectrometer [Rocha et al., 2018]. (b) Camera image for UV-Vis spectrometer (Varian Carry 4000 spectrometer).

Bandgap Calculation: The optical bandgap (E_g) of a semiconductor whether it is direct or indirect can be determined by using Tauc's plot[Klein et al., 2023; Tauc, 1968]. Here $(\alpha h\nu)^n$ is plotted vs. photon energy (E) and after extrapolating the linear region to the photon energy (E) axis an optical bandgap (E_g) of the material can be determined.

$$E(eV) = h\nu = \frac{hc}{\lambda} = \frac{1240}{\lambda\ (nm)} \qquad (2.7)$$

Where, α is the absorption coefficient (in cm^{-1} unit) of the material. n=2 for a material having direct bandgap and n=1/2 is used for a material having direct bandgap. Moreover, h and c are the plank's constant, whereas ν and λ are the frequency and wavelength of the photon energy.

Note: Absorbance is independent from the intensity of the source as we measure the ratio of I_o and I. We can work with optimum intensity of the source. Here, two detectors (in case of double beam spectrometer) are placed in front of source.

Sample Preparation: Thin films or drop casted were prepared over glass slides and measurements were performed using Varian Carry 4000 spectrometer in absorbance as well as reflectance mode.

2.11.2 Photoluminescence Spectroscopy

It is a spontaneous emission of light under band-to-band charge recombination from any semiconducting material after the absorption of light at a particular wavelength. The term luminescence is derived from a Latin word 'lumen' which means 'the process of' and hence refers to the process of emitting light. It is used to determine the bandgap of the material, recombination mechanism, purity, and phase of the material. The most frequent types of photoluminescence from a semiconductor are fluorescence and phosphorescence. Jablonski Diagram is the much more rigorous and complete diagram for summarizing photoluminescence (**Figure 2.17**).

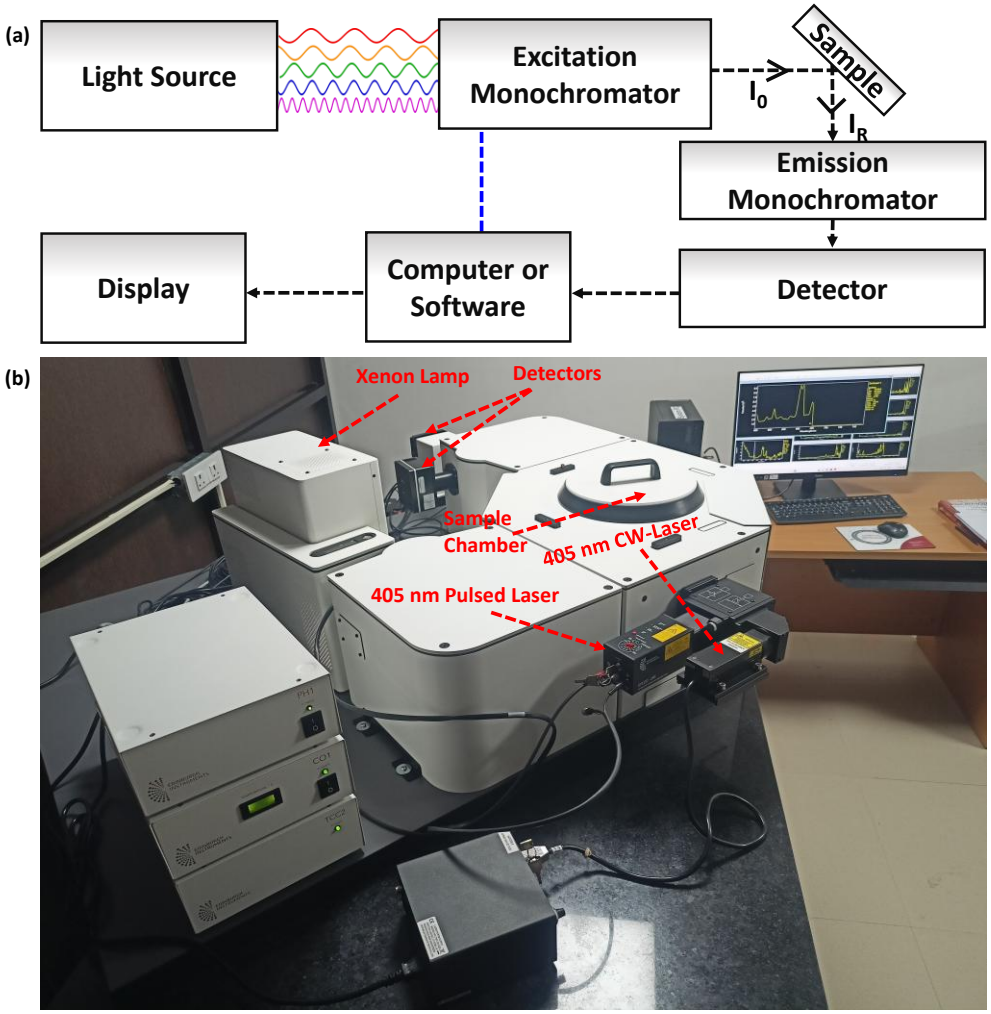


Figure 2.17 (a) Schematic representation showing the working principle of PL spectrometer. (b) Camera image for PL as well TRPL spectrometer integrated together (Edinburgh FLS1000).

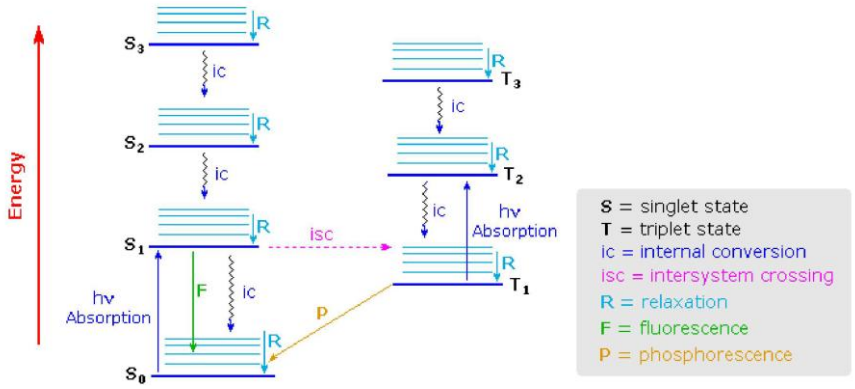


Figure 2.18 Jablonski Diagram showing Absorption, Emission (Fluorescence and Phosphorescence) ["https://www2.chemistry.msu.edu/faculty/reusch/virttxtjml/photchem.htm," n.d.].

When luminescence arises from an excited state that has same spin multiplicity as the ground state, as in the case of here, where both ground state and excited state are in singlet state (**Figure 2.18**). The electrons in the HOMO and LUMO are no longer in the same orbital and thus they no longer need to be opposite in spin. It is possible for the electrons on the LUMO to flip spins, resulting in a triplet state with two unpaired electrons. (Note: This is the simplified description. In reality triplet state is a combination of three microstates that comprise the S=1 triplet state).[S. Teets, 2021] Nevertheless, the process of changing spin multiplicity-in this state, singlet to triplet-is referred to intersystem crossing (ISC). It is also possible for luminescence to occur from the triplet state via radiative relaxation of the excited electrons from the LUMO back to the HOMO, with an accompanying spin flip to produce the singlet ground state. In this case, luminescence would be specifically termed as phosphorescence, which in a general sense is luminescence that involves a ground state and excited state with different multiplicities.

Process	Transition	Timescale (sec)
Light Absorption (Excitation)	$S_0 \rightarrow S_n$	ca. 10^{-15} (instantaneous)
Internal Conversion	$S_n \rightarrow S_1$	10^{-14} to 10^{-11}
Vibrational Relaxation	$S_n^* \rightarrow S_n$	10^{-12} to 10^{-10}
Intersystem Crossing	$S_1 \rightarrow T_1$	10^{-11} to 10^{-6}
Fluorescence	$S_1 \rightarrow S_0$	10^{-9} to 10^{-6}
Phosphorescence	$T_1 \rightarrow S_0$	10^{-3} to 100
Non-Radiative Decay	$S_1 \rightarrow S_0$ $T_1 \rightarrow S_0$	10^{-7} to 10^{-5} 10^{-3} to 100

Figure 2.19 Absorption and Emission Rate Comparison in Photoluminescence ["https://www2.chemistry.msu.edu/faculty/reusch/virttxtjml/photchem.htm," n.d.].

Note: (a) Fluorescence and Phosphorescence emission spectrum are obtained at longer wavelength as compared to the absorbance spectrum of same sample and the difference between absorbance and emission wavelength is called as stokes shift [Ahmad et al., 2014b; Blancon et al., 2018]. The fluorescence (nanosecond to picosecond) emission is a fast process as compared to phosphorescence (millisecond to 10^2 second) **(Figure 2.19)**.

(b) In photoluminescence spectrometer, the intensity of the emission spectrum is directly proportional to the intensity of the incident light on the sample[Tebyetekerwa et al., 2020] and a detector is placed at 90° to avoid the contamination of emitted light from the incident light as shown above **(Figure 2.20)**.

Sample Preparation: Thin films were prepared over glass slides and measurements were performed on LS 55 PerkinElmer fluorescence spectrometer coupled Xe-lamp.

2.11.3 Time Resolved PL Spectrometer

Time resolved photoluminescence spectroscopy is used to determine the charge carrier decay lifetime of a semiconductor. Photoluminescence decays often occur between 100 femtoseconds to nanoseconds, necessitating short light pulses and high temporal resolution instruments. The time-correlated single photon counting (TCSPC) approach is used to calculate photoluminescence lifetimes. Where, the probability of time distribution of a single emitted photon follows the statistical distribution of all the emitted photons and if we increase the similar experiments, then the probability distribution for the emission of all the single-photon occurrences reveals the intensity distribution over time for all the photons released. This approach has excellent temporal resolution, allowing for averaging across many events, and may be employed with very weak fluorophores. TCSPC uses several cycles of excitation and emission to produce an analogue voltage indicating optical flux even when the emitted light is not too strong. It uses repeating and accurate photon timing from a fluorescent sample. This requires a high photon repetition rate from

the excitation source. Pulse repetition rates are commonly 1–100 MHz and pulse lengths are femtoseconds to 100 picosecond. It also has nanosecond and picosecond time resolution.

A pulsed laser source (e.g., Titanium-Sapphire Laser, Diode Laser), monochromator, single photon detector, and fast TCSPC electronics (e.g., constant fraction discriminator; CFD, total amplitude converter; TAC, analog to digital converter; ADC, multi-channel analyzer; MCA) make up TCSPC. CFD collects exact timing information from trigger and detector in the TCSPC module, which is usually based on the TAC/ADC principle. The TAC effectively measures START and STOP pulse intervals and originates an analog output pulse proportionate to the time interval. This pulse is delivered to the ADC which provides a value to the corresponding time interval between the photon emitted and the excitation pulse. This time interval is assigned to channels of a MCA, which distributes and accumulates signals. If the emission light level is low, a single photon/cycle (one count) is detected in one MCA channel. After several counts, the time difference between each photon's START and STOP pulses forms a histogram of photon arrivals per channel. After "n" repetitions (typically 10,000 counts), a significant statistical distribution of counts as a function of channel number is achieved to correctly measure decay time.

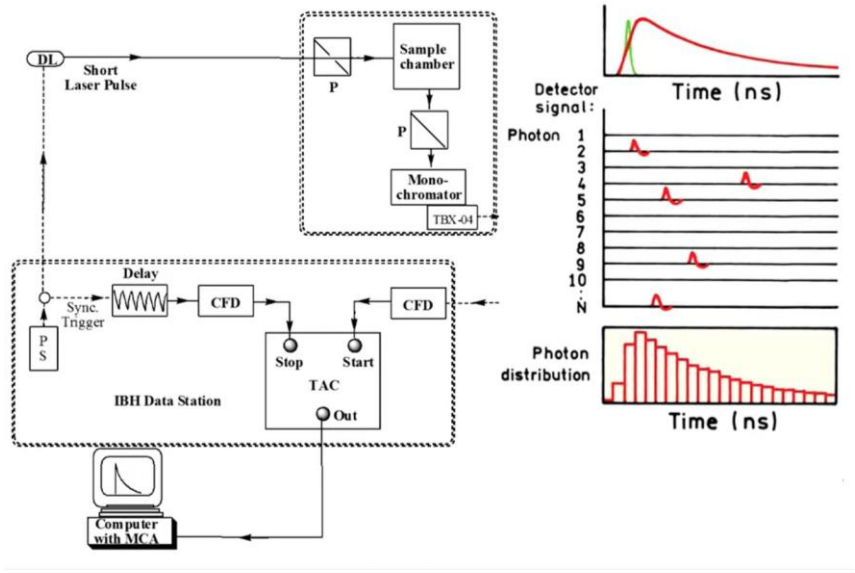


Figure 2.20 Schematic diagram showing the working mechanism of TRPL.

Average Decay Lifetime Calculation:
The decay profile vs. time of a semiconductor was obtained at a particular emission wavelength. The emission wavelength which is obtained from steady state PL. Double exponential expression (Y) is used to fit the decay profile.

$$Y = A_1 e^{\frac{-\tau}{\tau_1}} + A_2 e^{\frac{-\tau}{\tau_2}} \qquad (2.8)$$

Where, Y is the amplitude component. A_1 and A_2 are photoluminescence constants. τ are the time constant. τ_1 and τ_2 are the quicker and slower decay periods respectively. Moreover, the average decay lifetime τ_{avg} are calculated using following formula.

$$\tau_{avg} = \frac{A_1 {\tau_1}^2 + A_2 {\tau_2}^2}{A_1 \tau_1 + A_2 \tau_2} \qquad (2.9)$$

Sample Preparation: Thin films were prepared over glass slides and measurements performed on Horiba Delta Flex model using TCSPC method. Where, second harmonic (vertical polarization) of Mai Tai (resolution of the data acquisition: 13 ps per bin (channel), repetition rate: 8 MHz and TAC range: 100 ns) is used as excitation source.

2.12 Optoelectronic Characterizations

Optoelectronic performance such as current-voltage (I-V) characteristics and transient photocurrent (I-T) response of materials are recorded using photodetectors in vertical as well as lateral configuration. To investigate them, semiconducting material is coated (thin film or dropcasted) between two metal electrodes so that electron-hole pairs are generated in the photoactive material and extracted to the corresponding electrodes. Schematic and camera image for corresponding setup is shown in **figure 2.21a** and **figure 2.21b-c** respectively. Where, lateral photodetector is connected with Biologic VMP3 and 405 CW-Laser is used for illumination. Fabrication of photodetectors are mentioned in **Section 2.7**.

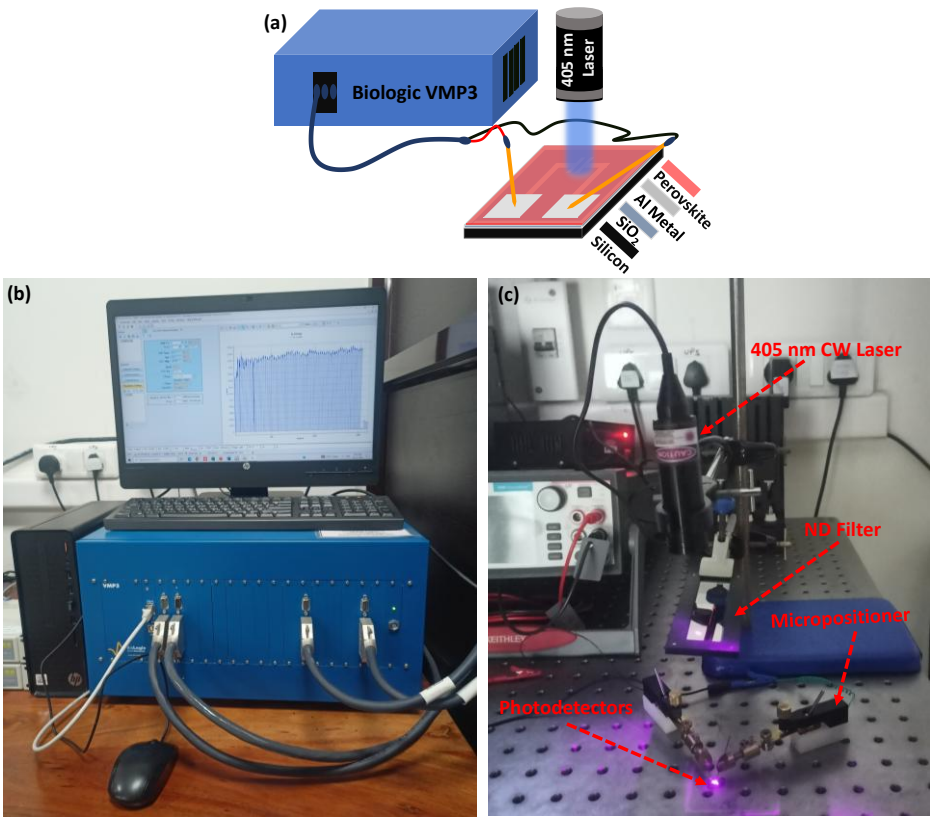


Figure 2.21 Schematic representation showing photodetection measurement setup used to measure photocurrent. (b) Camera image for Biologic VMP3 work station (c) Camera image for photodetector coupled through Biologic via micropositioner. 405 nm CW Laser is used for illumination and ND Filter is used to tune the incident illumination power.

2.12.1 Current-Voltage (I-V) Characteristics

It is defined as a relationship between direct current obtained from electronic device and direct voltage when applied across its terminals. I-V characteristic further categories below.

i. **Passive and Active:** The optoelectronic devices limited to the first and third quadrants of the I-V plane are called passive devices. In these devices, the electric current consistently flows in the direction of the electric field, namely from the positive terminal to the negative terminal so that charges lose their energy in the form of heat. That's why these devices consume power from circuits. Resistors and electric motors are common examples of passive devices. Batteries and generators are the common example of active devices which work opposite to the passive devices.

ii. **Linear and non-linear:** Linear I-V curves are represented by straight line. Both resistors and capacitors are linear devices, meaning that their resistance remains constant regardless of the applied voltage. Whereas non-linear I-V curves are represented by curved lines. A diode is

a straightforward example of a non-linear device in which the resistance changes with the supplied voltage.

2.12.2 Transient Photocurrent (I-T) response

It is a technique used to investigate the time dependent extraction of electron-hole pairs from semiconducting devices under illumination, which is responsible for the generation of photocurrent. This technique is recorded under bias conditions (i.e., V_{bias}= 0 V, ±1 V, … , V_{bias}<∞).

2.12.3 Different optoelectronic performance parameter for photodetector

The parameters to investigate the performance of a photodetector as shown in equations from **(2.10) to (2.14).**

i. **Dark Current (I_{dark}):** It is undesirable current that flows under dark conditions and has a negative impact on the performance of a photodetector. It is caused by leakage current, poor contact, an energy mismatch between the photoactive and transport layers, defects, and thermal noise [Li et al., 2020; Ollearo et al., 2021].

ii. **Photo Current (I_{light}):** It is desirable current that flows under light illumination and has positive impact on the performance of a photodetector. It is caused due to the generation of e-h pairs under illuminations.

iii. **Response Speed (τ_{rise}/τ_{decay}):** It is time required to rise (τ_{rise}) the photocurrent response from 10-90% under illumination and fall (τ_{decay}) from 90-10% under dark conditions.

iv. **Responsivity (R):** It shows the electrical current generated by a photodetector under per unit optical signal illumination on active area of device. It is defined as:

$$\mathbf{R} = \frac{\mathbf{I_{light} - I_{dark}}}{\mathbf{P_{in} \times S}}, \quad [\mathbf{A\,W^{-1}}] \tag{2.10}$$

v. **Detectivity (D):** It shows how well a photodetector can detect weak signal. It is defined as:

$$\mathbf{D} = \mathbf{R}\sqrt{\frac{\mathbf{S}}{\mathbf{2qI_{dark}}}}, \qquad [\mathbf{cm\,Hz^{\frac{1}{2}}/W}] \tag{2.11}$$

vi. **Noise Equivalent Power (NEP):** The NEP defines power generated in photodetector by noise source.

$$\mathbf{NEP} = \frac{\sqrt{\mathbf{S}}}{\mathbf{D}}, \qquad [\mathbf{W/Hz^{\frac{1}{2}}}] \tag{2.12}$$

vii. **External Quantum Efficiency (EQE):** The EQE defines the efficiency of a photodetector to convert incident photons into electrical charge carriers.

$$\mathbf{EQE}\ (\%) = \frac{\mathbf{1.24 \times 10^5 \times R}}{\boldsymbol{\lambda}}\ \% \tag{2.13}$$

viii. **ON-OFF ratio:** It shows the ability of photodetector to distinguish the signal in presence of light and baseline signal in dark.

$$\mathbf{ON - OFF\ Ratio} = \frac{\mathbf{I_{light}}}{\mathbf{I_{dark}}} \tag{2.14}$$

Where, S is the effective illumination area of the photodetector. λ is the wavelength of incident light and P_{in} is the incident optical power density. $q = 1.6 \times 10^{-19}$ coulomb denotes the charge of electron.

2.13 Electrochemical Techniques

It is an analytical that uses an electrochemical cell (Li-ion battery) to conduct chemical reactions involving electrical charges. Majorly, this technique includes cyclic voltammetry (CV), galvanostatic charging discharging (GCD) and electrochemical impedance spectroscopy (EIS). The camera image for electrochemical workstation setup is shown in **figure 2.22**. Whereas, the fabrication of LIBs electrodes and corresponding coin cells are mentioned in **Sub Section 2.13.4.** and **Sub Section 2.13.5**.

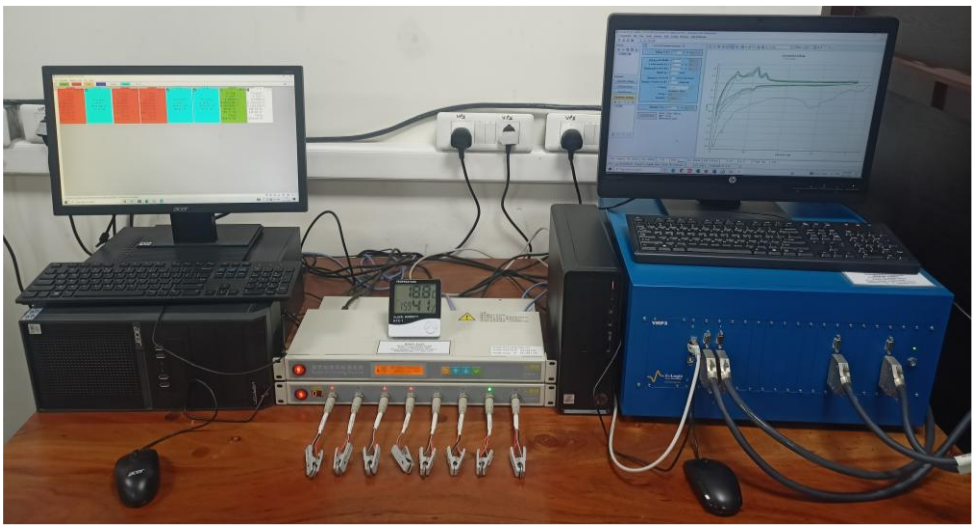


Figure 2.22 Electrochemical workstation setup (Left) Battery cycler and (Right) Biologic VMP3.

2.13.1 Cyclic Voltammetry (CV)

It involves the investigation of electrochemical reactions that occur at electrode-electrolyte interface. Here, electrode potential is swept linearly with time between potential limits V_1 and V_2 at a predetermined sweep rate, sometimes referred to as the scan rate. After reaching limit V_2, the sweep is reversed to V_1 to provide a cyclic scan. Such cyclic voltammogram has resulted in reduction-oxidation (redox) peak and the corresponding current is called redox current. In this thesis, CV were performed between V_1=0.02 V and V_2=2.00 V using Biologic VMP3 **(Figure 2.22)**.

2.13.2 Galvanostatic Charging-Discharging (GCD)

It is a technique to determine the performance of LIB. The purpose of the test is to figure out how many times a battery can be used before it begins to deteriorate after multiple cycles of charging and discharging. Here, LIB is charged and discharged galvanostatically within a predetermined potential range (V_1 and V_2) by applying constant current. In this thesis, GCD were performed between V_1=0.02 V and V_2=2.00 V using Biologic VMP3 and battery cycler both **(Figure 2.22)**.

2.13.3 Electrochemical Impedance Spectroscopy (EIS)

It is a technique for determining the kinetics and processes of electrochemical systems. To investigate the EIS, an AC signal of constant amplitude and variable frequency is supplied to the LIB. In this thesis, EIS were performed from 1 MHz to 0.01 Hz with voltage amplitude 10 mV.

R_s is a series combination resistance due to real impedance value at Z_{imag} = 0 Ω in the high-frequency region of the Nyquist plot, which is related to the current collector active material interface (CCAMI) and electrolyte resistance [Ventrapragada et al., 2018]. In addition, R_{ct} is the

resistance due to the characteristic semicircle in the mid of high-frequency regions, which is related to the charge transfer in the electrodes **(Figure 2.23)**.

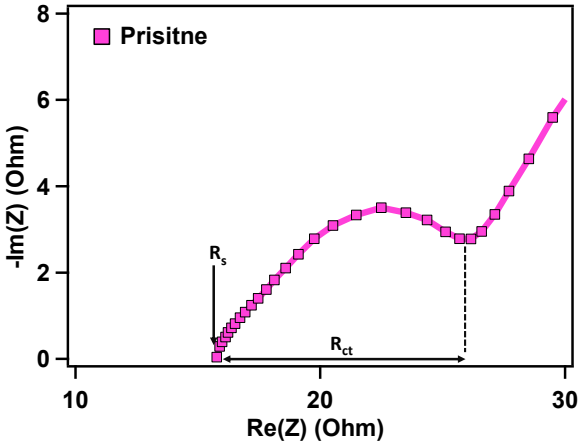


Figure 2.23 EIS plot for LIB showing R_s and R_{ct}.

In order to investigate these techniques, pristine and hybrid electrodes and then corresponding LIBs are fabricated as discussed below:

2.13.4 Fabrication of electrodes for pristine/hybrid LIBs



Figure 2.24 Camera image for Glove box from Vacuum Techniques Pvt Ltd.

The slurry for pristine electrodes were prepared by using 85 wt % mg pristine RP perovskite, 5 wt % reduced graphene oxide (rGO), 3 wt % carbon black powder (Super-P) and 7 wt % polyvinylidene difluoride (PVDF, Sigma Aldrich) in 1 ml N-Methyl-2-pyrrolidone (NMP). Whereas the slurry for hybrid electrodes were prepared by using 84.6 wt % pristine RP perovskite, 5 wt % reduced graphene oxide, 3 wt % carbon black powder and 7 wt % polyvinylidene difluoride in 1 ml solution of NMP with ~ 0.4 wt % MoS_2 nanoflakes. First, the mixture of rGO and carbon black powder is ultrasonicated in NMP for 1 hour followed by magnetic stirring for 48 hours to get uniform dispersion solution. Next, RP perovskite powder is added into the solution followed by magnetic stirring for 1 hour. Finally, PVDF binder was added to the solution, which was continuously magnetically stirred throughout the night to get uniform slurry. 20 µl solution was drop-casted on pre-cut circular Cu-foil (16 mm diameter, Alfa

Aesar). The electrodes are annealed overnight inside Ar-filled glove box at 70 °C to eliminate the NMP solvent. The effective mass loading of the active material is estimated to be ~ 1.7 mg.

2.13.5 LIB Fabrication

LIBs (coin cell-2032) are fabricated inside Ar-environment glove box system with less than 1 ppm oxygen and moisture levels to avoid degradation of the electrolyte (1M, $LiPF_6$, Alfa Aesar) and lithium metal **(Figure 2.24)**. First, the perovskite electrode prepared on Cu-foil is positioned in the middle of the positive casing, and then separator (19 mm diameter, glass microfibre) is placed on top of it. Subsequently, 30 µl of electrolyte is drop casted uniformly on separator. After that a counter electrode lithium metal foil is placed on top of electrolyte-soaked separator followed by stainless steel disk and a spring to compress the electrodes. Finally, negative top casing is placed and cell is assembled with the help of a mechanical hydraulic battery crimper (1000 psi). All the components required during the fabrication of LIBs are shown in **figure 2.25**.

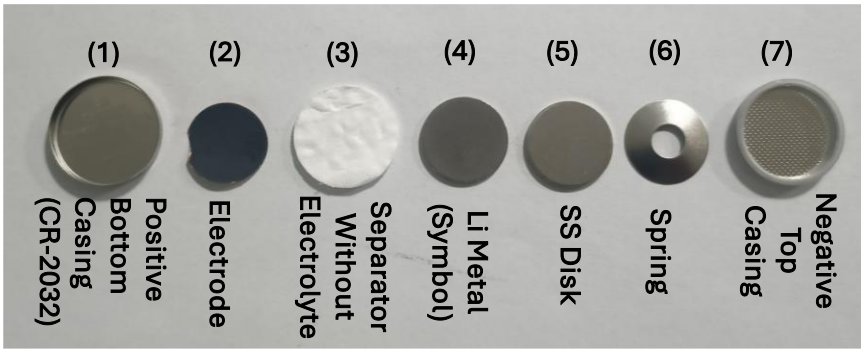


Figure 2.25 Different components of LIBs.

2.14 Photoelectrochemical Techniques

These techniques are similar to electrochemical techniques such as CV, and GCD, the only difference is that they are recorded under the illumination of light. In order to investigate these techniques, hybrid electrodes and then corresponding Li-LIBs are fabricated as discussed below:
The CV curves are recorded at a scan rate of 0.1 mV s^{-1} over 0.02 to 2.0 V voltage window under dark condition, and at a scan rate of 0.3 mV s^{-1} over 0.02 to 1.6 V voltage window under dark and illumination conditions using electrochemical workstation (Biologic VMP3). GCD measurements are performed at different specific current densities ranging from 58 to 76 mA/g under dark and illumination conditions over 0.02 to 1.6 V voltage window. For these measurements, a white LED light (12 mW/cm^2) is used as illumination source. In addition to that, OCV charging (without applying any constant current density; under illumination) measurements are recorded by measuring open circuit voltage response using 1 Sun illumination (Xe-lamp, 100 mW/cm^2), for 0.05-1.35 V voltage window, as well as under LED (12 mW/cm^2), for 0.06-0.47 V, voltage window illumination and discharged galvanostatically by applying discharge current density.

2.14.1 Fabrication of electrodes for hybrid Li-PRBs

The slurry for pristine electrodes were prepared by using 85 wt % mg pristine RP perovskite, 5 wt % rGO, 3 wt % carbon black powder (Super-P) and 7 wt % PVDF in 1 ml NMP. Whereas the slurry for hybrid electrodes were prepared by using 84.6 wt % pristine RP perovskite, 5 wt % reduced graphene oxide, 3 wt % carbon black powder and 7 wt % polyvinylidene difluoride in 1 ml solution of NMP with ~ 0.4 wt % MoS_2 nanoflakes. First, the mixture of rGO and carbon black powder is ultrasonicated in NMP for 1 hour followed by magnetic stirring for 48 hours to get uniform dispersion solution. Next, RP perovskite powder is added into the solution followed by magnetic stirring for 1 hour. Finally, PVDF binder was added to the solution, which was continuously magnetically stirred throughout the night to get uniform slurry. 20 µl solution was drop-casted on pre-cut circular Cu-foil (16 mm diameter) / FTO (1 x 1.5 cm^2, thickness ~ 2.3 mm, ~ 13 Ω sq^{-1}) with extended Cu-foil to make electrodes. The electrodes are annealed overnight inside Ar-filled glove box at 70 °C to eliminate the

NMP solvent. The effective photoactive area of PRB is kept as 1×1 cm^2 and effective mass loading of the active material is estimated to be ~ 1.7 mg.

2.14.2 Li-PRB Fabrication

Li-PRBs are fabricated in an Ar-filled glovebox with less than 1 ppm oxygen and moisture levels. First Al foil strip, stainless steel (SS) disc and then Li metal foil (15 mm in diameter) are placed on the top of glass slide (2.6×3.9 cm^2). Subsequently, a separator (glass microfibre Whatman paper) soaked in 30 µl electrolyte (1M $LiPF_6$) is placed on top of the Li metal foil, followed by the photoelectrode (prepared on FTO with extended Cu-foil). In order to keep all layers together, a second glass slide is positioned on top of the photoelectrode. Finally, the edges are sealed completely, and clips are applied to preserve the interfacial connections between all components.

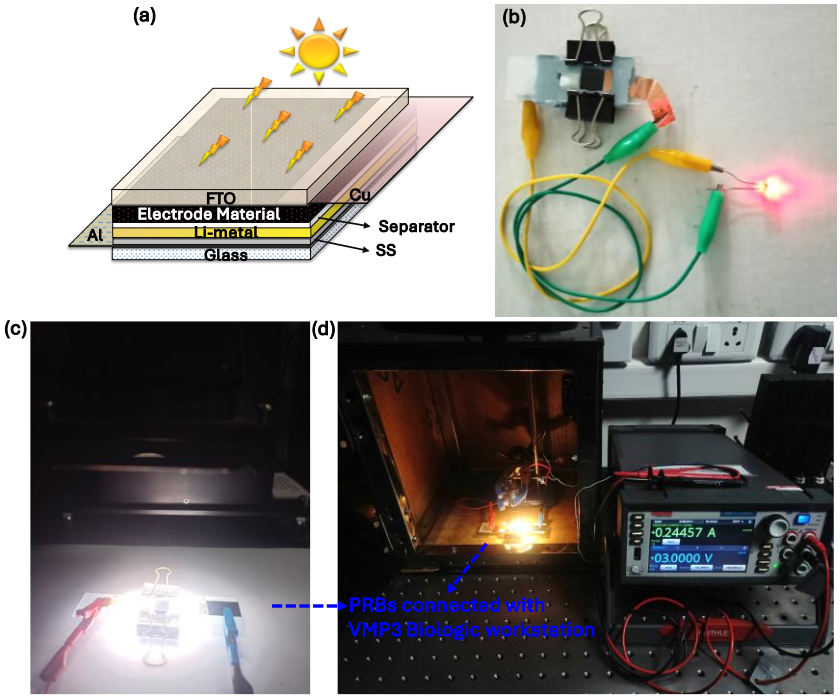


Figure 2.26 (a) Schematic diagram for Li-PRB. (b) Camera image for Li-PRB powering LED. Camera image showing Li-PRB connected with Biologic with (c) 1 Sun illumination and (d) Warm LED light (12 mW/cm^2) is illuminations on the Li-PRB. Complete setup is enclosed in the light enclosure.

2.13.3 Photoconversion and Storage Efficiency (PC-SE) calculations

PC-SE is defined as the ability of a PRB for the conversion and then storage of incident optical power in the form of electrochemical energy simultaneously. The calculations for photo conversion and storage efficiency (PC-SE), η of Li-PRBs.

$$\eta\,(\%) = \frac{E_{Discharge}}{P_{in} \times t_{OCV} \times A_{illu}} \times 100 \qquad (2.15)$$

Where, $E_{Discharge}$ denotes the discharge energy, P_{in} denotes incident power density, t_{OCV} denotes OCV charging (without adding any constant current; under illumination conditions only) time, A_{illu} denotes illuminated area of the photoelectrode.

$$P_{in} = 100\,mW cm^{-2}\ (For\ 1\ Sun\ illumination, Xenon - Lamp)$$

$$P_{in} = 12\,mW cm^{-2}\ (For\ White\ LED\ illumination)$$

....